Functionalizing DNA nanostructures with natural cationic amino acids

Dong Wang [a,e,1], Chunfa Chen [a,1], Qian Liu [b], Qianwen Zhao [a], Di Wu [a], Yue Yuan [a], Chaowang Huang [a], Xiaorong Sun [a], Chunji Huang [c], David Tai Leong [d,***], Guansong Wang [a,**], Hang Qian [a,*]

[a] *Institute of Respiratory Diseases, Xinqiao Hospital, Third Military Medical University, 183 Xinqiao Street, Chongqing, 400037, China*
[b] *Laboratory of Pharmacy and Chemistry, And Laboratory of Tissue and Cell Biology, Lab Teaching & Management Center, Chongqing Medical University, Chongqing, 400016, China*
[c] *Basic Medical College, Third Military Medical University, Chongqing, 400038, China*
[d] *Department of Chemical and Biomolecular Engineering, National University of Singapore, Singapore*
[e] *Department of Respiratory Medicine, Jinling Hospital, Nanjing, Jiangsu, 210002, China*

ARTICLE INFO

ABSTRACT

Complexing self-assembled DNA nanostructures with various functional guest species is the key to unlocking new and exciting biomedical applications. Cationic guest species not only induce magnesium-free DNA to self-assemble into defined structures but also endow the final complex nanomaterials with new properties. Herein, we propose a novel strategy that employs naturally occurring cationic amino acids to induce DNA self-assembly into defined nanostructures. Natural L-arginine and L-lysine can readily induce the assembly of tile-based DNA nanotubes and DNA origami sheets in a magnesium-free manner. The self-assembly processes are demonstrated to be pH- and concentration-dependent and are achieved at constant temperatures. Moreover, the assembled DNA/amino acid complex nanomaterials are stable at a physiological temperature of 37 °C. Substituting L-arginine with its D form enhances its serum stability. Further preliminary examination of this complex nano-material platform for biomedical applications indicates that DNA/amino acids exhibit distinct cellular uptake behaviors compared with their magnesium-assembled counterparts. The nanomaterial mainly clusters around the cell membrane and might be utilized to manipulate molecular events on the membrane. Our study suggests that the properties of DNA nanostructures can be tuned by complexing them with customized guest molecules for a designed application. The strategy proposed herein might be promising to advance the biomedical applications of DNA nanostructures.

1. Introduction

Self-assembled DNA nanostructures with excellent programmability, biocompatibility, and versatility are highly promising nanomaterial platforms in nanomedicine. Nevertheless, naked DNA nanostructures are prone to be digested by cell lysates in a 3- to 24-h time window depending on the structural design [1–5], thus circulating for a very short time in mouse blood. The vulnerability of DNA nanostructures in physiological environments and the lack of cost-effective conjugation of arbitrary functional moieties substantially limit their biomedical

applications. The global surface of most DNA nanostructures is negatively charged and leaves very few options for functionalization. Moreover, the delivery efficiency of DNA nanostructures in naturally negatively charged biological systems presents another challenge. These challenges greatly hinder the overall practical applications of DNA nanostructures. Thus far, few studies have attempted to overcome these issues. Shih et al. reported a method to protect DNA nanostructures by covering them with a layer of oligolysine [6]. The serum and structural stabilities of DNA nanostructures were significantly improved. Similarly, Kostiainen and Hernandez-Garcia et al. covered a DNA origami

sheet with a layer of proteins [7,8]. Schmidt et al. reported that covering DNA nanostructures with a polymer layer provided promising protection [9]. Other strategies, such as engineering sequence-defined peptoids, have also been proposed to protect DNA nanostructures [10]. A few strategies have been explored to decorate naked DNA nanostructures with drugs or other functionalities. The most commonly reported methods are the direct intercalation of guest molecules such as doxorubicin and porphyrin [11,12] and hybridization with siRNA [13, 14], miRNA or aptamers [15,16]. Chemical modification is another important decoration method. Zhang et al. substituted nucleosides with floxuridine, thus making a drug out of DNA [17]. Gothelf et al. covalently attached DNA with peptides and proteins to mimic IgM [18]. Although the chemical modification approach is tedious, less cost-effective than other methods, and requires a sophisticated design, it indeed expands the DNA nanostructure applications. Other strategies, such as combining DNA nanotechnology and host/guest chemistry for hybrid nanostructure construction, have also been reported [19–21]. Collectively, biomedical applications of DNA nanostructures are rapidly increasing and show promising potential in drug delivery, biosensing, bioimaging, and biological catalysis [22–26]. The engineering techniques to create functional DNA nanomaterials need to meet the demand of these fast-growing expectations.

Self-assembly of DNA nanostructures with functional guest species and subsequently into complex nanomaterials is a highly promising way to endow DNA nanostructures with desired functionalities. Conventionally, DNA nanostructures are synthesized in neutral or slightly basic aqueous buffers in the presence of Mg^{2+}. The synthesis mediator Mg^{2+} is crucial to maintain structural integrity but has a negligible contribution to potential applications. A few studies have demonstrated that DNA self-assembly in a magnesium-free manner is feasible. Simmel et al. demonstrated that polyamines could mediate DNA origami self-assembly [27]. Keller et al. reported that DNA origami structures were stable at low Mg^{2+} concentrations even in Mg^{2+}-free conditions [28]. Additionally, it was reported that nitrogen-enriched carbon quantum dots with a small size of approximately 2 nm could facilitate DNA prism self-assembly [14]. The synthesized hybrid nanomaterial possessed potential in cancer theranostic applications. These studies suggested that it is feasible and highly desirable to synthesize DNA nanostructures with guest molecules in a magnesium-free manner to obtain complex nanomaterials with new properties.

Drawing inspiration from physiological insights that circulating DNA is robust enough to be used as a biomarker in cancer diagnosis and that
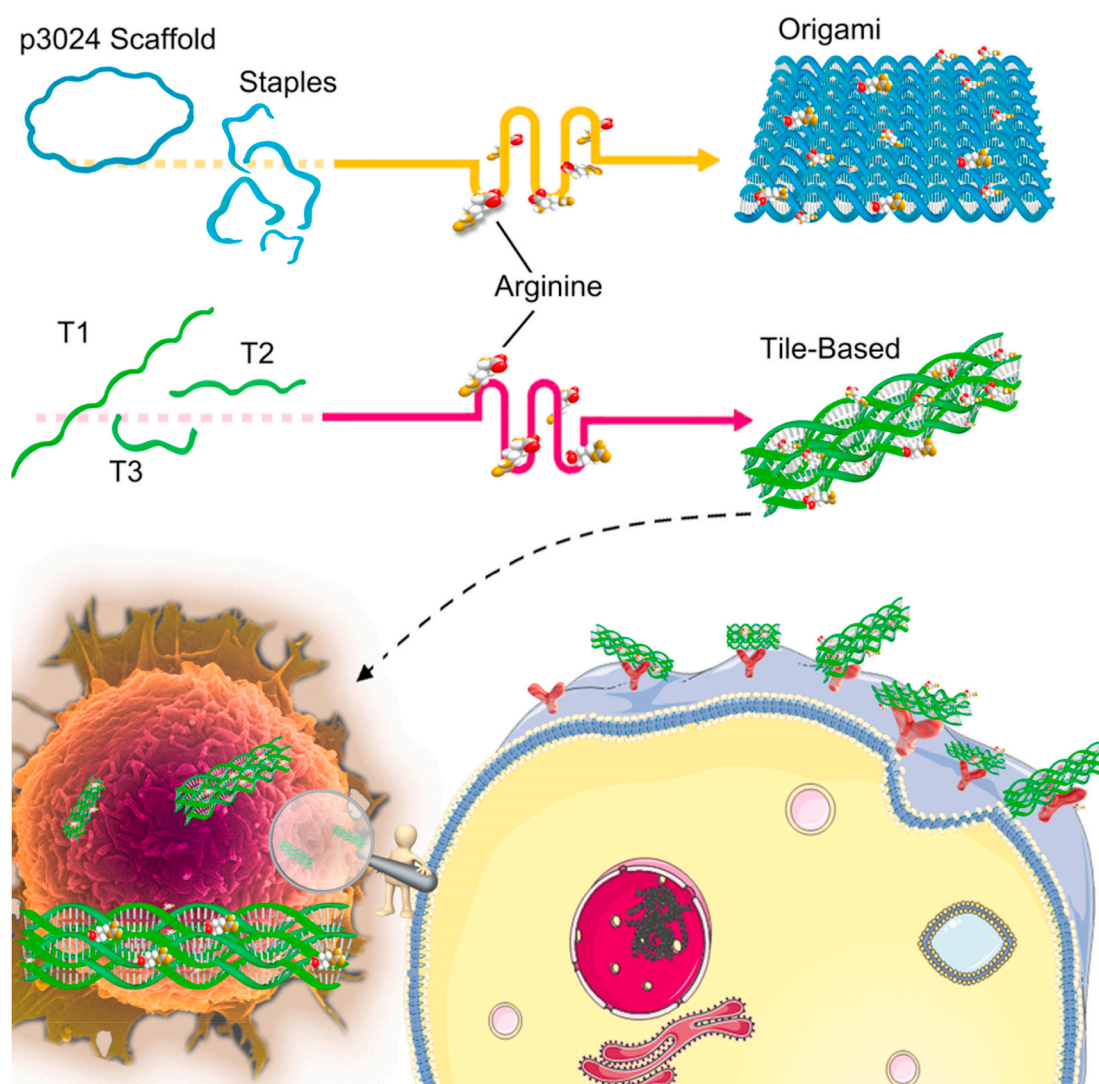
Fig. 1. Cationic amino acids induce DNA self-assembly and their interactions with cells. DNA nanotube and DNA origami sheet structures were utilized to validate the DNA self-assembly. DNA origami sheets have lengths and widths of 52 and 32 nm, respectively. Three short DNA strands of T1, T2, and T3 hybridize with each at a molar ratio of 2:6:6 to form a tubular structure. Arginine is selected to represent the three cationic amino acids (arginine, lysine, and histidine). Arginine/DNA complex nanomaterials interact with cancer cells by aggregating on cell membranes, possibly through surface receptors.

the stability of DNA is enhanced by bound proteins such as nucleosomes [29], we proposed that natural single amino acids can directly result in dual *de novo* assembly and stabilization of novel DNA nanostructures. Essential amino acids such as arginine, lysine, and histidine are the three positively charged amino acids at a neutral pH with pK_a values of 10.76, 9.74, and 7.59, respectively. At approximately physiological pH 7.0, the guanidine or amine group of the three amino acids is protonated and thus can neutralize DNA during self-assembly and sustain the stability of the as-formed structure in a biologically pH neutral microenvironment. Additionally, complexing DNA nanostructures with amino acids may endow the obtained nanomaterial with pH responsiveness by switching the system pH.

In this study, we explored the potential of cationic amino acids in the self-assembly of DNA nanotubes and origami sheets (Fig. 1). The DNA nanotube was designed and constructed by a tile-based strategy [30]. It is composed of three different short DNA strands and has a length and diameter of 13.8 and 6.0 nm, respectively (similar to a 6-helix bundle). A DNA origami sheet was designed with a size of 52 × 32 nm using the p3024 scaffold. The self-assembly behaviors, complex nanostructure stability, and biocompatibility were thoroughly investigated by polyacrylamide gel electrophoresis (PAGE), atomic force microscopy (AFM), dynamic light scattering (DLS), and confocal laser scanning microscopy (CLSM). We demonstrated that arginine and lysine could successfully induce the self-assembly of both structures. The hybrid nanomaterial can be synthesized isothermally or by stepwise annealing in high yields. The complex nanomaterial showed interesting new properties compared with Mg^{2+}-assembled DNA nanostructures. When arginine was substituted with its D-form, the as-assembled complex nanoparticles exhibited higher serum stability. Moreover, the hybrid nanoparticles were mostly located on the cancer cell membrane. This phenomenon, together with the high serum stability, indicated that self-assembly of DNA nanostructures with functional guest species is indeed an excellent way to engineer functional DNA nanomaterials for potential biomedical applications and for use in other research fields [31–34].

2. Materials and methods

2.1. Materials

Short DNA oligos were obtained from Sangon Biological Engineering (Shanghai, China) and used as received (ultraPAGE purified). Cy5-tagged probes were synthesized and purified by HPLC (Sangon, China). The p3024 scaffolds were purchased from Bioruler, China. L and D forms of arginine, lysine, histidine, 40% acryl/bis solution (19:1), Tris, EDTA, acetic acid, magnesium acetate, formamide, DNA Ladder, Stains-all, Gelred (BBI), and Hoechst 33342 were acquired from Sangon (Shanghai, China). Dii was obtained from Sigma Aldrich (USA). Modified Eagle's medium (MEM), RPMI-1640 medium, fetal bovine serum (FBS), and trypsin (0.25%) were obtained from Gibco (USA).

DNA sequences can be found in the Supporting Information.

2.2. Synthesis of DNA nanostructures

Synthesis of DNA nanotubes. The component DNA strands T1, T2, and T3 were mixed at a molar ratio of 1:3:3 in pure amino acid solutions before being subjected to the annealing process. Other than amino acids, DNA, and ultrapure water, no other ingredients were involved in the synthesis system. Mg^{2+}-assembled DNA nanotubes were synthesized in Tris-acetic-EDTA-Mg^{2+} (TAE/Mg^{2+}) buffer (pH 8.0). The DNA nanotube concentrations were kept at 330 nM. The amino acid concentrations (final concentration in each sample) varied from 40 to 450 mM depending on the experimental settings. For DNA origami sheets, the scaffold concentrations of different samples were kept at 50 nM. The DNA scaffold and staple ratios varied from 1:1 to 1:10 according to the experimental settings. The mixtures were then subjected to the following annealing process: 95 °C/5 min, 65 °C/30 min, 50 °C/30 min,

37 °C/30 min, and 22 °C/30 min. For isothermal self-assembly, the mixtures were incubated at constant temperatures for 3 h.

2.3. PAGE and agarose gel electrophoresis

The DNA nanostructures were analyzed by 6% PAGE (diluted from 40% 19:1 acrylamide/bis acrylamide) and 2% agarose gels. Gels were run on a Bio-Rad Electrophoresis System (USA) at room temperature for 1–3 h at a constant voltage of 65 or 120 V. For running buffer, TAE/Mg^{2+} was used, and the gel was stained with Stains-all solution (0.01%) or gelred. The extracellular stability of D-form amino acid/DNA complex nanostructures was evaluated by native PAGE. Approximately 2 μg nanomaterials in solution were incubated with 10% FBS for different time points at 37 °C and then run with PAGE.

Stability assay of DNA nanostructures: The thermal stability of arginine- and lysine-assembled DNA nanotubes was analyzed by 6% PAGE in an electrophoresis unit (Bio-Rad) at 37 °C (constant voltage, 125 V) for 30 min. Arginine and lysine concentrations were 300 mM for DNA self-assembly. The pH values for the arginine and lysine synthesis systems were 7.0 and 8.0, respectively. DNA nanostructures assembled with different synthesis mediators were incubated with 10% FBS and PBS and then incubated at 37 °C for serial durations (0, 6, 12, 24, and 36 h). The samples were prepared in 300 mM L/D arginine, L/D lysine, and 1X TAE/Mg^{2+} buffer. The stability of the samples was then characterized by 6% PAGE in a Hoefer SE 600 Chroma Vertical Electrophoresis System at room temperature (constant voltage, 250 V) for 1 h. A 0.01% 'Stains-All' solution was employed to stain the gels for 2 h before scanning by an HP scanner.

Buffer exchange with spin columns: The spin column with a cut-off molecular weight of 100 K was first washed with ultrapure water at 5000 RPM centrifugation. After that, 60 μL of DNA solution was added to the tube first, and then 300 μL washing buffer arginine (2 mM) or water was added to the tube. Centrifuge it at a speed of 3000 RPM for 5 min until the remaining solution in the upper tube was approximately 60 μL. Repeat the washing process thrice. Collect the DNA samples for PAGE gel electrophoresis.

2.4. Cell culture

A549 cells were cultured in RPMI-1640 medium. The media contained 10% fetal bovine serum (FBS), 100 units mL^{-1} penicillin, and 100 μg mL^{-1} streptomycin. These cells were grown in a 95% humidified atmosphere of 5% CO_2 at 37 °C. The cells were trypsinized and counted before each experiment when they grew to 80%–90% confluence.

2.5. AFM imaging and DLS measurements

For AFM imaging, a 5 μL DNA sample solution was dropped onto a freshly cleaved mica surface and incubated for 5 min to allow for strong adsorption. The sample drop was then washed off using 50 μL ultrapure water and dried by compressed nitrogen. The DNA nanostructures were then imaged by AFM under scanaysist-air mode using a Multimode 8 AFM system (Bruker, USA) with silicon tips on nitride levers (T: 650 nm, L: 115 μm, W: 25 μm, f0: 70 kHz, k: 0.4 N/m). The tip-surface interaction was minimized. The DNA nanostructure solution was diluted to ~100 nM for DNA nanotubes and 10 nM for origami sheets. Samples were then measured by DLS (Malvern Instruments Laser Target Designator, UK).

2.6. CLSM imaging, flow cytometry, and MTT assay

For confocal microscopy, cells were cultured in a 24-well plate, with a coverslip over each well, overnight at a density of 1×10^4 cells/cm^2 under standard culture conditions. Then, the cells were treated with Cy5-labeled DNA nanotubes (strand T3 was replaced with Cy5-labeled strand T3-Cy5) for 12 or 24 h. The cell received Cy5 concentration was 300 nM. Mg-NT and Ar-NT concentrations were 50 nM. No

transfection agents were used. The volume ratio between the DNA sample and medium was 1:9. After the treatment, the cells were stained with Hoechst 33342 dye (final concentration: 1 μg mL^{-1}) for 30 min, washed with PBS buffer 5 times, and fixed with a mixture of 4% paraformaldehyde for 15 min. Finally, the cells were washed with PBS buffer 3 times before imaging by an inverted microscope (Nikon ECLIPSE TS100).

Flow cytometry: Cells were cultured in a 6-well plate overnight at a density of 2×10^4 cell/cm^2 and incubated with Cy5-labeled DNA nanotubes for 12 h. The Cy5 fluorophore and DNA nanotube concentrations were kept at 300 and 50 nM. After incubation, cells were then digested by trypsin and collected in PBS buffer with 2% FBS. The collected cells were collected and washed with PBS thrice. Cells were then resuspended in 350 μL of PBS and used for flow cytometry (Backman, Gallios, USA).

MTT assay: Amino acids and DNA nanotubes assembled with arginine (300 mM, Ar-NT), lysine (300 mM, Lys-NT), and Mg^{2+} (1X TAE/Mg^{2+} buffer, Mg-NT) were prepared prior to the experiment. A549 cells
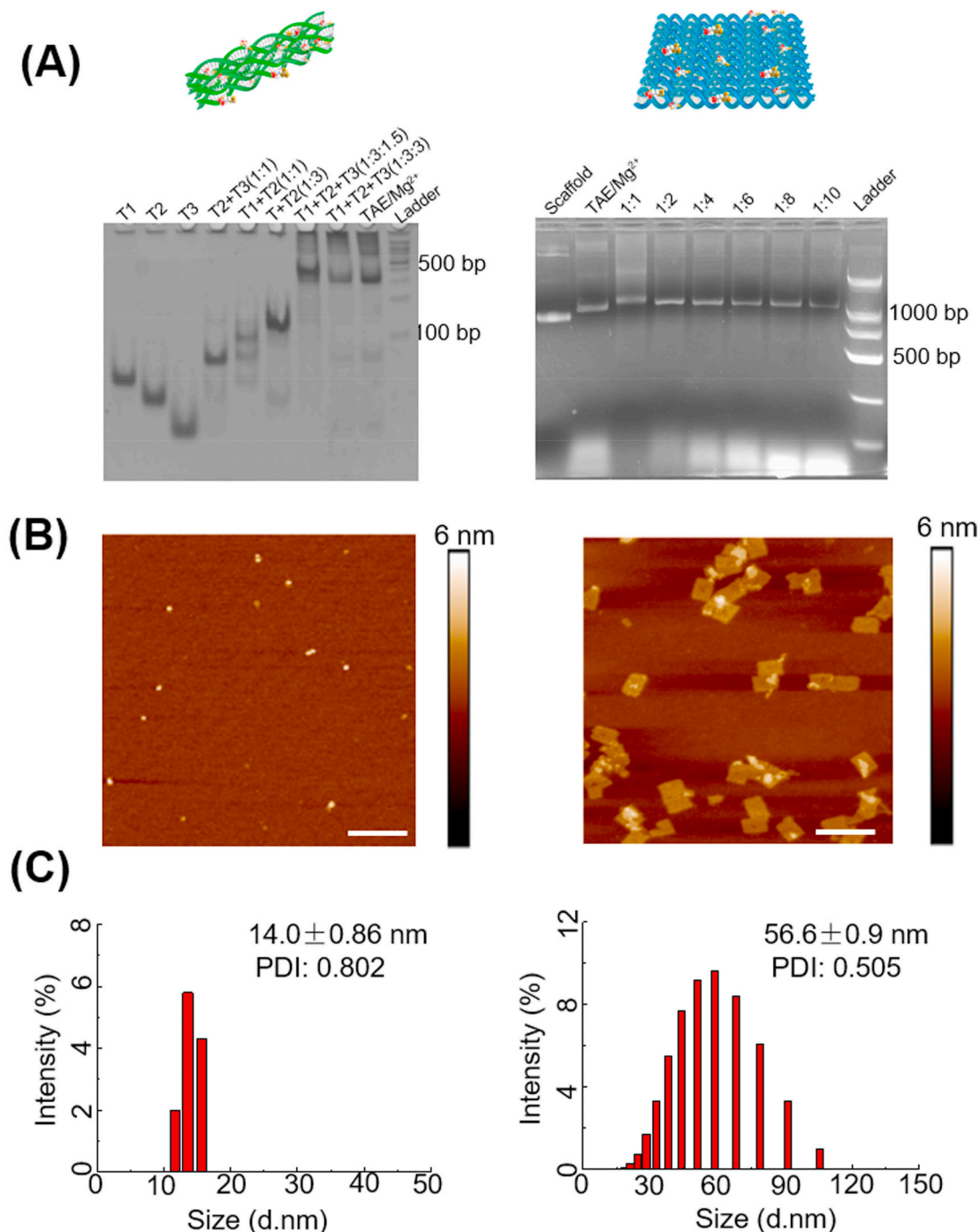
Fig. 2. Synthesis and characterization of arginine-assembled DNA nanotubes and origami sheets. (A) PAGE and agarose gel electrophoresis showed the formation of both structures. Scaffold-to-staple ratios are indicated on the agarose gel. (B) AFM imaging of arginine-assembled DNA nanotubes and DNA origami sheets. The DNA nanotube and origami sheets were assembled at arginine concentrations of 300 and 200 mM, respectively. The pH values of both synthesis systems were 7.0. The scaffold/staple ratio was 1:4. The DNA nanostructures were purified before imaging. Scale bar: 100 nm. (C) DLS measurements of the size of the two structures. The synthesis system was kept at pH 7.0.

were cultured in a 24-well plate for 12 h. Then, the cells were incubated with arginine, lysine, Mg-NT, Ar-NT, and Lys-NT separately for another 24 h. Sample and medium volume ratios were kept at 1:9. Cells that received arginine/lysine received a concentration of 30 mM.

3. Results and discussion

3.1. Design of the functionalization of self-assembled DNA nanostructures with cationic amino acids

DNA self-assembly relies on the neutralization of the negative charge carried by the phosphonate group. Conventionally, DNA nanostructures are assembled in Mg^{2+}-containing buffer (TAE/Mg^{2+}). In the current study, we proposed that cationic amino acids, such as arginine and lysine, might be able to induce DNA self-assembly in a Mg^{2+}- free manner. The two fundamental DNA self-assembly strategies, tile-based, and square lattice-based 2D DNA origami, are tested. Arginine and lysine are naturally existing endogenous biomolecules. Living organisms have developed sophisticated machinery to process these molecules. However, as the component elements in DNA/amino acid complex nanomaterials, how cationic amino acids affect the surface properties of complex nanoparticles and subsequently their interactions with

biosystems such as cells remain elusive. As shown in Fig. 1, both DNA origami and tile-based structures are assembled with arginine or lysine in a Mg^{2+}-free system. The interactions between the obtained DNA/ amino acid complex nanostructures and cells are investigated. These natural endogenous biomolecules containing complex nanomaterials may have potential in the fields of drug delivery, bioimaging, and sensing.

3.2. Synthesis and characterization of arginine-induced DNA nanostructures

We first evaluated the potential of arginine in magnesium-free self-assembly. As shown in Fig. 2A, the formation of DNA nanotubes and origami sheets was analyzed by PAGE and agarose gel electrophoresis. Different DNA strand combinations of DNA nanotubes appeared as clear intermediate product bands with reasonable mobilities on the gel. The final nanotube structures exhibited a sharp, concentrated band located between the 300–400 bp region of the DNA ladder, which is comparable with its molecular weight. DNA nanotubes synthesized with TAE/Mg^{2+} were also examined by PAGE (Fig. S1). As expected, the two gels exhibited similar patterns. The DNA origami sheet band had a clear shift compared to the p3024 scaffold and Mg^{2+}-assembled counterparts. No
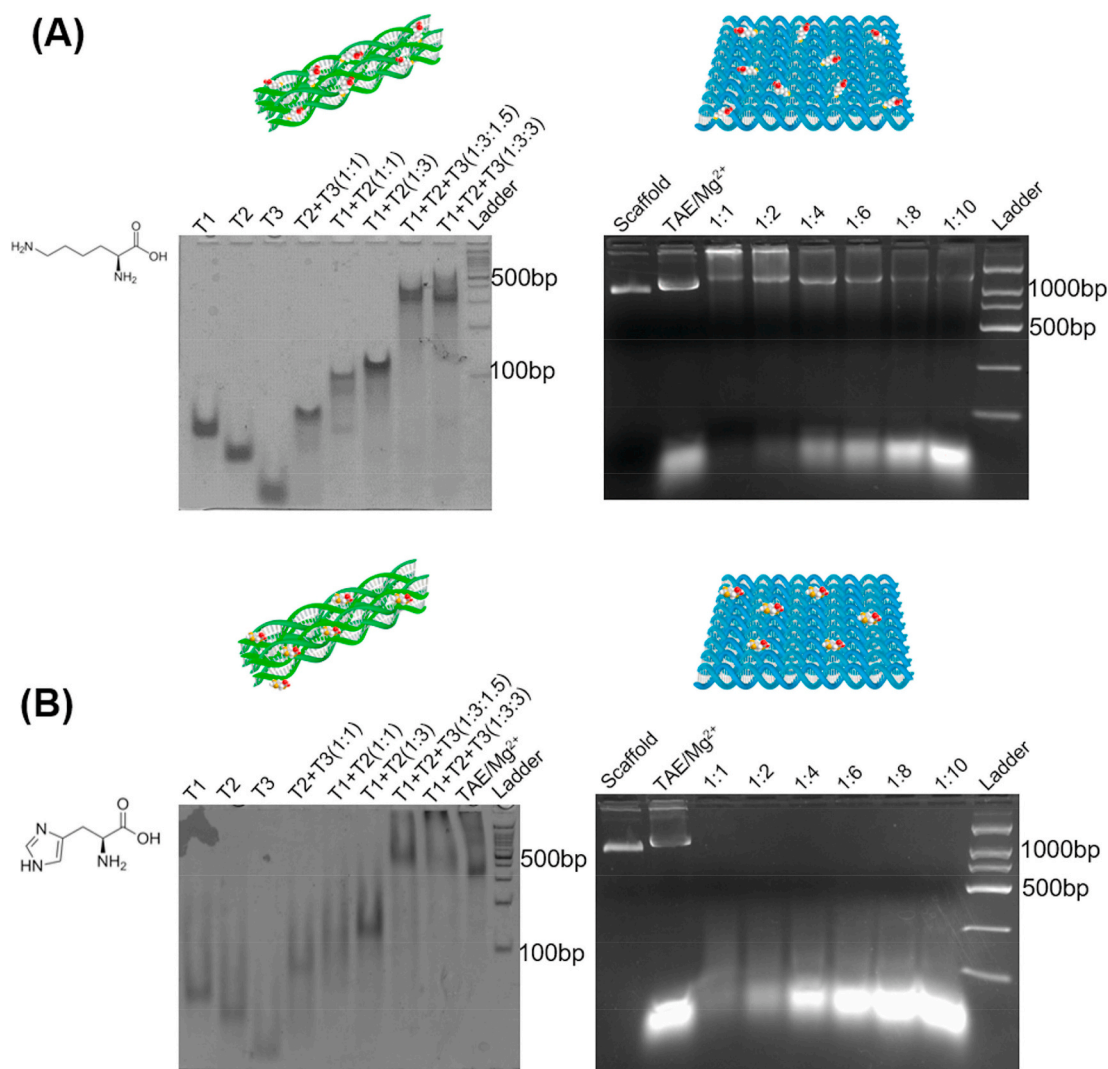
Fig. 3. DNA self-assembly with lysine and histidine. (A) PAGE and agarose gel electrophoresis of lysine-assembled DNA nanostructures. The lysine concentrations for self-assembly were 250 and 300 mM for DNA nanotubes and origami sheets, respectively. The system pH was kept at 8.0. (B) PAGE and agarose gel electrophoresis showed the capability of histidine to assemble DNA nanostructures. Due to the poor solubility of histidine in water, saturated histidine solutions (~270 mM) were utilized for the self-assembly of both structures. The pH value of the histidine system is lower than 7.0, as indicated by the pH test strips.

dominant bands were formed in the absence of arginine and Mg^{2+} (Fig. S2). Strong evidence of DNA nanotube and origami sheet formation came from AFM imaging (Fig. 2B). DNA nanotubes exhibited discrete, uniformly dispersed nanoparticles on the mica surface. Rectangularly shaped sheets were clearly observed with appropriate size. Height analysis indicated that the heights of both structures matched well with their theoretical designs (Fig. S3). AFM imaging of DNA origami sheets with different scaffold/staple ratios was also examined (Fig. S4). We

further demonstrated arginine-synthesized DNA nanostructure formation with DLS (Fig. 2C). The hydrodynamic diameters of the DNA nanotubes and origami sheets were 14.0 ± 0.86 and 56.6 ± 0.90 nm, respectively. Autocorrelation curves of the DLS measurements for both structures were shown in Fig. S5. These values were comparable to their designed lengths of 13.9 (nanotube) and 52 nm (origami sheet). These results suggested that arginine indeed induced the self-assembly of defined DNA nanostructures in the absence of Mg^{2+}.
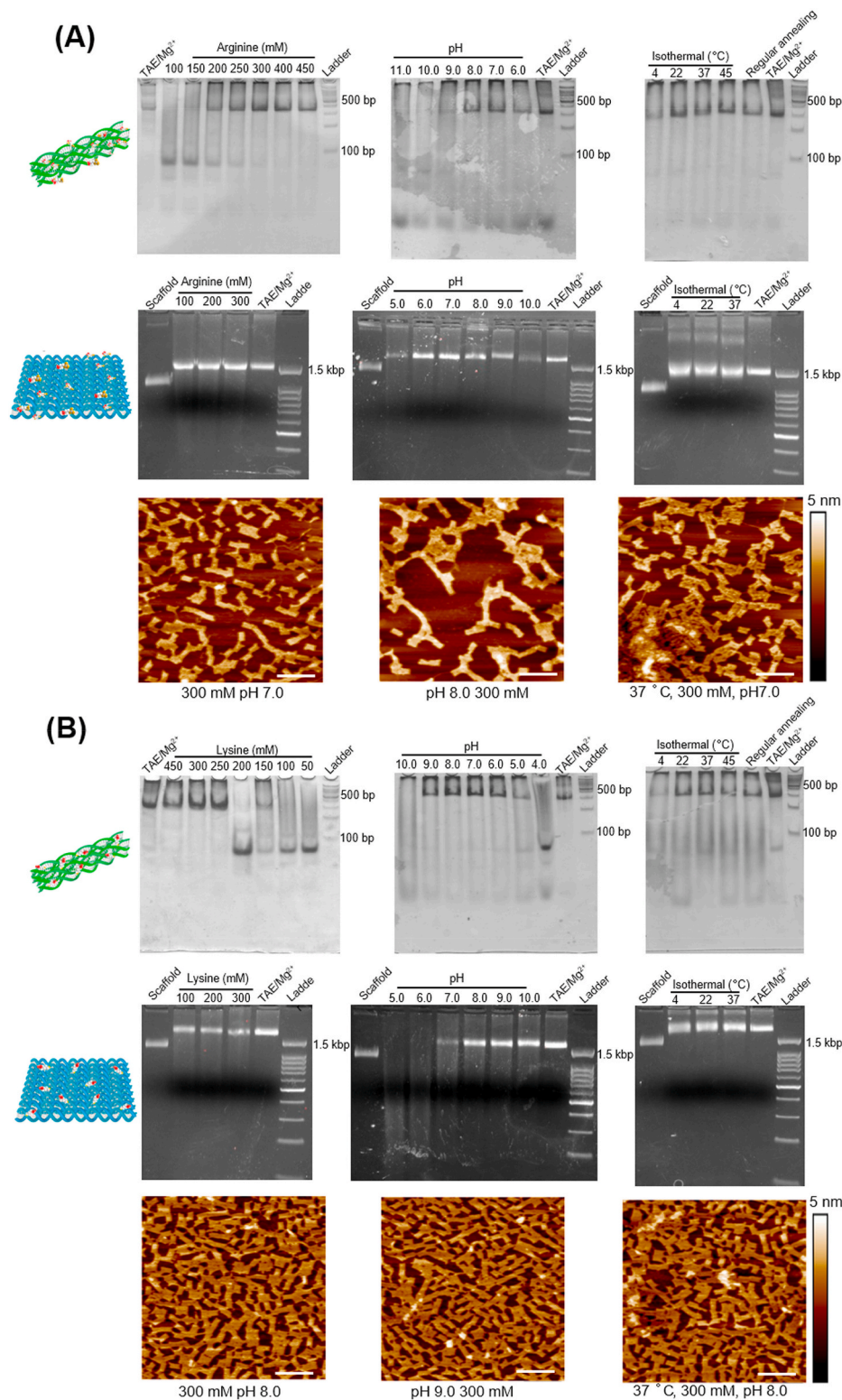
Fig. 4. Self-assembly behaviors of arginine- and lysine-induced DNA self-assembly. (A) PAGE and agarose gel electrophoresis of arginine-induced DNA nanotubes and DNA origami self-assembly. Upper panel: the concentration-, pH-, and isothermal temperature-dependent self-assembly behaviors of the DNA nanotubes; middle panel: the concentration-, pH-, and isothermal temperature-dependent self-assembly behaviors of origami sheets. Lower panel: AFM imaging of the assembled DNA origami sheets. The preparation conditions of the samples were labeled below the images. Scale bar: 200 nm. (B) DNA nanotubes and origami sheets were assembled by lysine at different concentrations, pH values, and temperatures. AFM imaging was also conducted to confirm origami sheet formation. Scale bar: 200 nm.

3.3. Investigation of lysine- and histidine-induced DNA self-assembly

Lysine and histidine are two positively charged amino acids at neutral pH. PAGE indicated that DNA nanotubes were assembled by lysine in high yields (Fig. 3A). DNA origami sheets with different scaffold/staple ratios were also present on the agarose gel. The gel electrophoresis of different component strand combinations exhibited similar patterns to those of arginine assembled combinations. Unfortunately, histidine failed to induce DNA origami assembly and induced DNA nanotube formation with a very low yield (Fig. 3B). We speculated that histidine might be poorly protonated at neutral pH because of the small pKa. Extra nitrogen-containing groups such as amine and guanidine in amino acids are responsible for DNA self-assembly since the main obstacle for DNA self-assembly is to overcome the negative charge repulsion. Primary amines or guanidine are highly polarized at an appropriate pH. We reasoned that other cationic guest molecules bearing similar groups with appropriate sizes might also be able to induce DNA self-assembly.

3.4. Arginine- and lysine-induced DNA self-assembly behaviors and mechanism

Next, we investigated arginine- and lysine-induced DNA self-assembly behaviors. The effects of the concentration, pH, and isothermal temperature on arginine-induced DNA nanostructure self-assembly were evaluated (Fig. 4A). The PAGE results indicated that the yield of DNA nanotubes reached its highest at an arginine concentration of 300 mM. A lower arginine concentration resulted in a lower yield or failure of DNA nanotube synthesis. DNA nanotubes could be synthesized with high yields from pH 6.0 to 8.0. Although arginine is positively charged at pH 9.0, the yield is very low. This was probably attributed to the insufficient protonation state of arginine. It was interesting that DNA nanotubes were successfully assembled by incubation with arginine at 4, 22, 37, and 45 °C for 3 h. The yield of DNA nanotubes at 4 °C was relatively lower than that at other temperatures, probably due to the slow kinetics at lower temperatures. The wide pH range and isothermal self-assembly ability suggested that arginine-induced DNA nanotube assembly was robust. For the DNA origami sheet, origami sheets assembled with different arginine concentrations exhibited similar mobilities on the agarose gel. However, AFM imaging indicated that origami sheets were formed only at arginine concentrations higher than 200 mM (Fig. S6). Isothermal self-assembly of origami sheets by arginine was only achieved at 37 °C. The products assembled at 4 and 22 °C moved slightly slower than those assembled at 22 °C and Mg^{2+}, indicating an incomplete structure. No intact rectangular shapes were observed under AFM. Additionally, DNA origami sheets could be assembled from pH 6.0 to 9.0, with its highest yield at pH 7.0 (Fig. S6). The optimal synthesis concentration, isothermal assembly temperature, and pH were different for the DNA nanotubes and origami sheets, which was most likely because of their different structural designs. Similarly, the self-assembly properties of lysine and DNA were also evaluated (Fig. 4B). Lysine could induce DNA nanotube and origami sheet assembly at minimum concentrations of 250 and 300 mM, respectively. The lysine-induced DNA self-assembly pH windows for DNA nanotubes and origami sheets were 6.0–9.0 and 7.0–9.0, respectively. The DNA origami sheet required a higher lysine concentration for self-assembly than the DNA nanotube, probably because the total numbers of negative charges of DNA are larger. When the system pH was below 7.0, DNA origami sheet yields quickly dropped, and large aggregates formed, which indicated that the acidic environment might provide a more positively charged environment that favored random DNA aggregation. Lysine-induced DNA nanotube and origami sheet isothermal self-assembly was also achieved. DNA nanotubes were formed at 22, 37, and 45 °C. For origami sheets, AFM imaging results showed that they were isothermally assembled at 22 and 37 °C (Fig. S7). The above-mentioned results suggested that both arginine and lysine are excellent

cationic guest species and readily mediate DNA self-assembly under mild conditions. Isothermal self-assembly of DNA is an interesting characteristic that may be applied in certain temperature-sensitive scenarios. It was reported that successful isothermal activity highly depends on the DNA sequences, structural design, and surrounding synthesis environments [35–37]. In the current study, both DNA nanotubes and origami sheets were relatively simple designs. Positively charged amino acids at constant temperatures for a sufficiently long time allowed for the error correction of strand hybridization toward designed superstructures.

It is worth noting that the required arginine and lysine concentrations are much higher than the theoretically calculated values for both structures. For example, DNA nanotubes (654 bases) require 654 positive charges, which equals 0.216 mM arginine or lysine, assuming that each bears one positive charge below their pK$_a$. It is well recognized that Mg^{2+} mostly resides at the major and minor grooves of the DNA duplex. For cationic species other than metal ions, their interaction mechanisms with DNA are rarely reported. Markvoort et al. simulated the interaction model between a series of small molecules and DNA nanostructures [38]. Larger molecules, such as peptides, mainly interacted with the phosphate backbone with one duplex or between two DNA duplexes. Arginine and lysine are larger than Mg^{2+}, and it is probably thermodynamically unfavorable for them to embed in the major grooves due to molecular constraints. The binding mode external to DNA grooves is less precise and thus may require more arginine and lysine. Another possible reason may be that the guanidine and amine groups in arginine and lysine interacted with DNA bases through hydrogen bonding, which depleted a significant number of amino acids. Nonetheless, the detailed binding modes between these three cationic amino acids and DNA during and after assembly require more investigation.

In addition to metal cations, polyamines, and amino acids, DNA self-assembly in denaturing environments (aqueous) or nonaqueous solvents represents another Mg^{2+}-free DNA self-assembly strategy. It was reported that DNA nanostructures based on DNA origami and SST could be assembled in aqueous solutions by controlling the concentrations of denaturing agents such as formamide and urea [39,40]. Interestingly, DNA origami assembly was also achieved in anhydrous solvents [41]. Instead of neutralizing negatively charged DNA with cationic species, the abovementioned studies realized defined DNA self-assembly by adjusting the surrounding environments and the denaturing status of DNA. Collectively, the underlying mechanism of Mg^{2+}-free DNA self-assembly was either substituting conventional Mg^{2+} with other cationic species or controlling the chemical properties of the assembly systems. It is anticipated that other DNA nanostructures with similar tile-based and 2D origami designs based on square lattice might also be amenable for arginine- and lysine-induced self-assembly by adjusting the system pH, concentration, and annealing protocols.

3.5. Stability of arginine- and lysine-assembled DNA nanostructures

Stability and biocompatibility are the primary concerns before applying amino acid-assembled DNA nanostructure complex nanomaterials to any potential biomedical applications. To investigate these properties, an arginine-assembled DNA nanotube (Ar-NT) was employed for proof-of-concept studies. We first tested the stability of Ar-NT at 37 °C. Fig. 5A shows the arginine- and lysine-assembled Ar-NT. Both Ar-NTs formed sharp bands with reasonable mobilities on the gel. Buffer exchange postassembly indicated that Ar-NTs were stable after being washed with low concentrations of arginine (2 mM) or ultrapure water (Fig. 5B). Further serum stability results showed that both Ar-NT (in L form) and Mg^{2+}-assembled DNA nanotube stability was reasonably long for within 6 h. However, it appears that in serum, there are proteases that can degrade L-Arg. We searched D-Arg, the nonnative version of Arg, and surprisingly, the serum stability of Ar-NTs was significantly improved. The Ar-NTs could last up to 24 h and partially exist even at 36 h. It was reported that D-amino acid substitution improved the
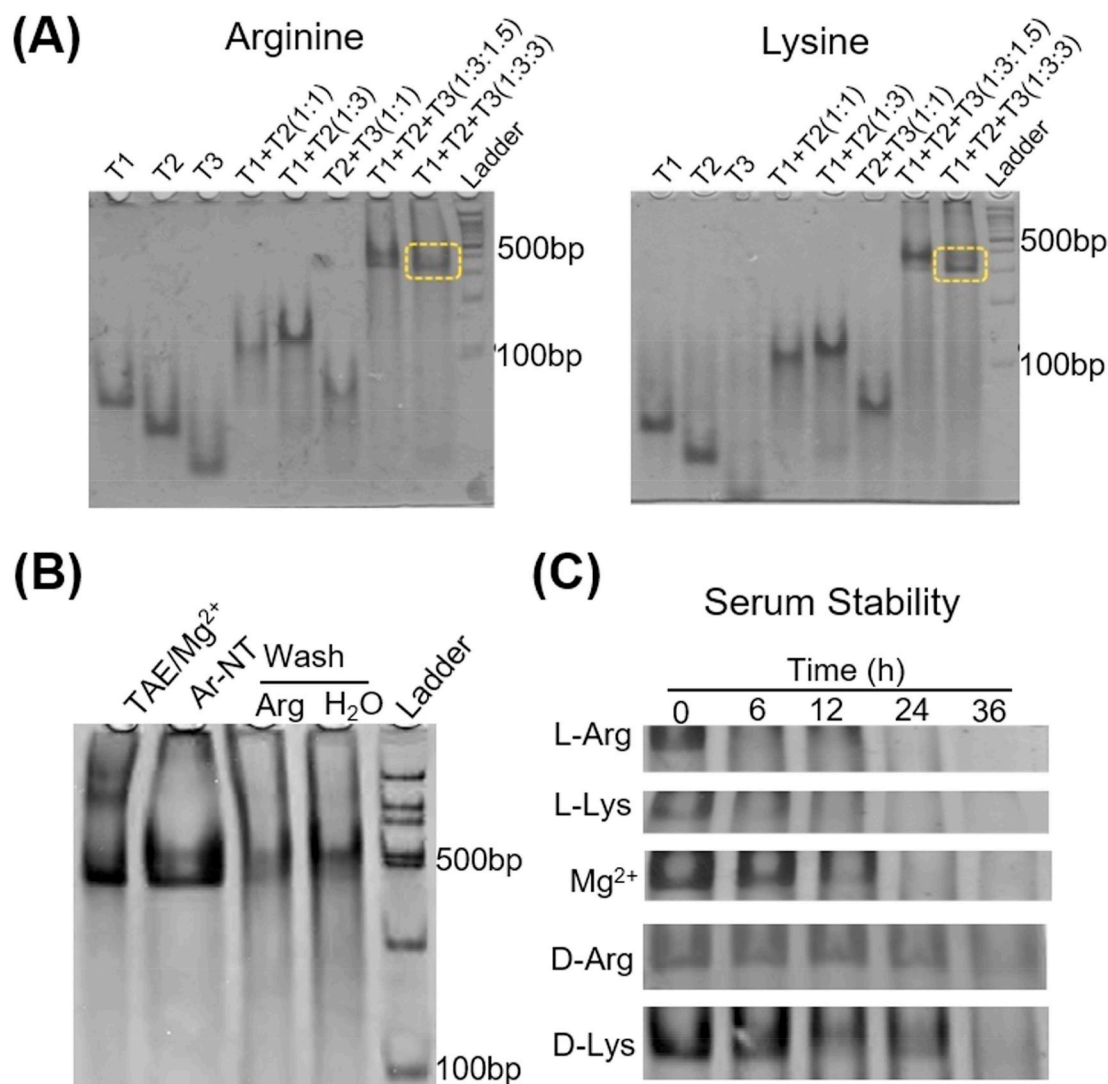
Fig. 5. Stability of arginine-assembled DNA nanotubes. (A) PAGE analysis of the formation of arginine- (left) and lysine- (right) assembled DNA nanotubes at 37 °C. (B) PAGE gel analysis of the arginine-assembled DNA nanotube stability examined by buffer exchange using spin columns. (C) Time course serum stability of L- and D-arginine-, L- and D- lysine-, and Mg^{2+}-assembled DNA nanotubes examined by PAGE.

enzymatic stability and binding affinity of peptides [42,43]. The D-amino acids in the complex DNA nanomaterials in our case might have a higher binding force to DNA and protease-resistant performance than L-amino acids. In addition, the biocompatibility of the complex nanomaterials was examined by MTT assay (Fig. S8). No cytotoxicity was observed under the current experimental conditions. The facile synthesis and high structural and serum stability laid a strong foundation for future applications of amino acid-DNA complex nanomaterials. The simple tunability of the stability of the DNA nanostructures allows both extremes of the translational window to be achieved without requiring the nanostructures to be redesigned.

3.6. Arginine-DNA complex nanoparticles interact with cells

To explore the interactions between Ar-NT and the cell interface, we conducted CLSM imaging experiments.

Mg-NT was also prepared and examined as a control. It was found that Ar-NTs mainly surrounded the cell membranes (Fig. 6A). Nevertheless, Mg^{2+}-assembled nanotubes (Mg-NT) were taken up into the cytoplasm and displayed as red dots around the nucleus. Quantification analysis by flow cytometry indicated that the red fluorescence signal of Ar-NT was 7.5-fold higher than that of Mg-NT (Fig. S9). We further

stained the cell membrane (green color) and found that the red fluorescence emitted by Ar-NT colocalized with the cell membrane very well and displayed a yellow color (Fig. 6B). Additionally, the accumulation of Ar-NT on the membrane increased with time. These distinct cellular uptake phenomena between Ar-NT and Mg-NT suggested that the arginine in Ar-NT altered the nanostructure surface properties compared with traditional Mg-NT. This colocalization may arise from the interaction between arginine in the complex and the cell receptor CATs (Cationic Amino Acid Transporters) [44]. Nonetheless, the detailed mechanism needs further investigation. These results demonstrated the advantages of assembling DNA nanostructures with cationic guest species. Future work using Ar-NTs and other amino acid-assembled DNA nanostructures to manipulate molecular events on the cell membrane is promising.

4. Conclusions

In this study, we proposed a DNA self-assembly strategy using cationic amino acids to assemble defined DNA nanostructures and obtain complex DNA nanomaterials to expand the biomedical applications of DNA nanostructures. Specifically, we reported that cationic arginine and lysine could induce DNA nanostructure self-assembly in a
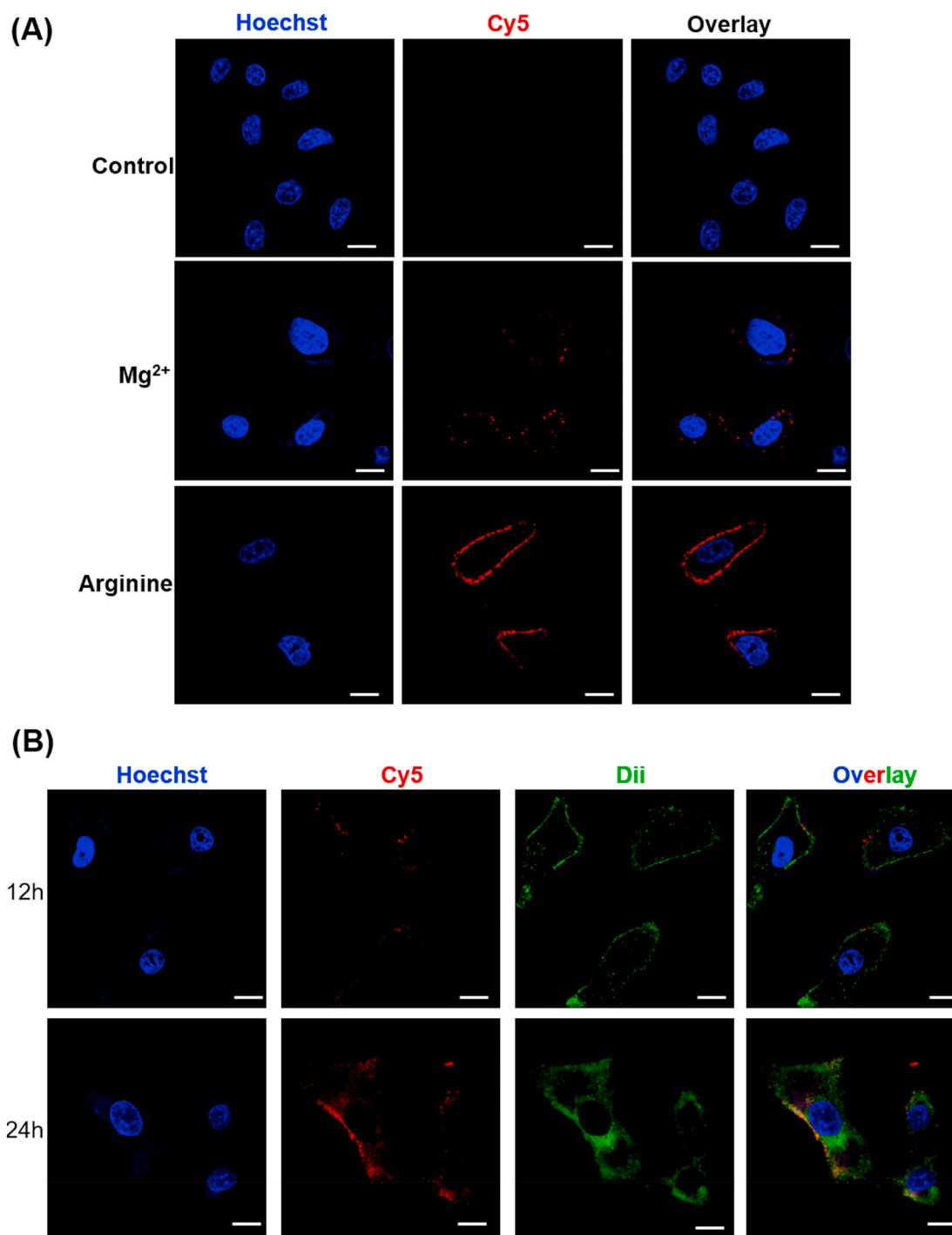
Fig. 6. CLSM imaging of the cellular uptake of arginine-DNA nanotube complex nanoparticles. (A) The cellular uptake of Mg-NT and Ar-NT was examined by CLSM. DNA nanotube was tagged with Cy5. The incubation time was 12 h, and the Cy5 concentrations were kept at 300 nM. (B) Colocalization of Cy5-labeled DNA nanotubes and A549 cell membranes. The cell membrane was stained with green dye. Arg-NTs were incubated with cells for 12 and 24 h at a Cy5 concentration of 300 nM. Scale bar: 20 μm.

magnesium-free system. The amino acid/DNA complex nanomaterials exhibited high structural and serum stability. Compared to Mg^{2+}-assembled DNA nanomaterials, the complex nanomaterials displayed distinct nanoparticle and cell interface properties. Additionally, the abundant amino and carboxyl groups in the complex nanomaterials provide more chances for further functionalization [45]. These new findings may present an approach for developing functional nanomaterials that complex DNA with natural biomolecules for biomedical applications.

CRediT authorship contribution statement

Dong Wang: Methodology, Formal analysis, Investigation. **Chunfa Chen:** Methodology, Formal analysis, Investigation. **Qian Liu:** Methodology, Investigation, Writing. **Qianwen Zhao:** Investigation. **Di Wu:** Investigation. **Yue Yuan:** Investigation. **Chaowang Huang:** Investigation. **Xiaorong Sun:** Supervision, Resources. **Chunji Huang:** Supervision, Resources. **David Tai Leong:** Conceptualization, Review & editing, Funding acquisition. **Guansong Wang:** Conceptualization, Supervision,

Funding acquisition. **Hang Qian:** Conceptualization, Supervision, Writing – review &editing, Funding acquisition.

Declaration of competing interest

There are no conflicts of interest to declare.

Acknowledgments

Appendix A. Supplementary data

Supplementary data to this article can be found online at https://doi.org/10.1016/j.bioactmat.2021.02.012.

References

[1] A. Lacroix, E. Vengut-Climent, D. Rochambeau, H.F. Sleiman, Uptake and fate of fluorescently labeled DNA nanostructures in cellular environments: a cautionary tale, ACS Cent. Sci. 5 (2019) 882–891.

[2] J.W. Conway, C.K. McLaughlin, K.J. Castor, H.F. Sleiman, DNA nanostructure serum stability: greater than the sum of its parts, Chem. Commun. 49 (2013) 1172–1174.

[3] J. Hahn, S.F. Wickham, W.M. Shih, S.D. Perrault, Addressing the instability of DNA nanostructures in tissue culture, ACS Nano 8 (2014) 8765–8775.

[4] D. Wang, Q. Liu, D. Wu, B. He, J. Li, C. Mao, G. Wang, H. Qian, Isothermal self-assembly of spermidine–DNA nanostructure complex as a functional platform for cancer therapy, ACS Appl. Mater. Interfaces 10 (2018) 15504–15516.

[5] X. Shen, Q. Jiang, J. Wang, L. Dai, G. Zou, Z.G. Wang, W.Q. Chen, B.Q. Ding, Visualization of the intracellular location and stability of DNA origami with a label-free fluorescent probe, Chem. Commun. 48 (2012) 11301–11303.

[6] N. Ponnuswamy, M.M.C. Bastings, B. Nathwani, J.H. Ryu, L.Y.T. Chou, M. Vinther, W.A. Li, F.M. Anastassacos, D.J. Mooney, W.M. Shih, Oligolysine-based coating protects DNA nanostructures from low-salt denaturation and nuclease degradation, Nat. Commun. 8 (2017) 15654.

[7] H. Auvinen, H. Zhang, Nonappa, A. Kopilow, E.H. Niemela, S. Nummelin, A. Correia, H.A. Santos, V. Linko, M.A. Kostiainen, Protein coating of DNA nanostructures for enhanced stability and immunocompatibility, Adv. Healthc. Mater. 6 (2017) 1700692.

[8] E.G. Sanchez-Rueda, E. Rodriguez-Cristobal, C.L. Moctezuma Gonzále, A. Hernandez-Garcia, Protein-coated dsDNA nanostars with high structural rigidity and high enzymatic and thermal stability, Nanoscale 11 (2019) 18604–18611.

[9] N.P. Agarwal, M. Matthies, F.N. Gür, K. Osada, T.L. Schmidt, Block copolymer micellization as a protection strategy for DNA origami, Angew. Chem. Int. Ed. Engl. 56 (2017) 5460–5464.

[10] S.T. Wang, M.A. Gray, S. Xuan, Y. Lin, J. Byrnes, A.I. Nguyen, N. Todorova, M. M. Stevens, C.R. Bertozzi, R.N. Zuckermann, O. Gang, DNA origami protection and molecular interfacing through engineered sequence-defined peptoids, Proc. Natl. Acad. Sci. U.S.A. 117 (2020) 6339–6348.

[11] V. Bagalkot, O.C. Farokhzad, R. Langer, S. Jon, An aptamer-doxorubicin physical conjugate as a novel targeted drug-delivery platform, Angew. Chem. Int. Ed. Engl. 45 (2006) 8149–8152.

[12] R.J. Fiel, J.C. Howard, E.H. Mark, N. Datta Gupta, Interaction of DNA with a porphyrin ligand: evidence for intercalation, Nucleic Acids Res. 6 (1979) 3093–3118.

[13] H. Lee, A.K.R. Lytton-Jean, Y. Chen, K.T. Love, A.I. Park, E.D. Karagiannis, A. Sehgal, W. Querbes, C.S. Zurenko, M. Jayaraman, C.G. Peng, K. Charisse, A. Borodovsky, M. Manoharan, J.S. Donahoe, J. Truelove, M. Nahrendorf, R. Langer, D.G. Anderson, Molecularly self-assembled nucleic acid nanoparticles for targeted in vivo siRNA delivery, Nat. Nanotechnol. 7 (2012) 389–393.

[14] D. Wu, B.L. Li, Q. Zhao, Q. Liu, D. Wang, B.F. He, Z.H. Wei, D.T. Leong, G.S. Wang, H. Qian, Assembling defined DNA nanostructure with nitrogen-enriched carbon dots for theranostic cancer applications, Small 16 (2020), e1906975.

[15] H. Qian, C.Y. Tay, M.I. Setyawati, S.L. Chia, D.S. Lee, D.T. Leong, Protecting microRNAs from RNase degradation with steric DNA nanostructures, Chem. Sci. 8 (2017) 1062–1067.

[16] H.M. Meng, H. Liu, H. Kuai, R. Peng, L. Mo, X.B. Zhang, Aptamer-integrated DNA nanostructures for biosensing, bioimaging and cancer therapy, Chem. Soc. Rev. 45 (2016) 2583–2602.

[17] Q. Mou, Y. Ma, G. Pan, B. Xue, D. Yan, C. Zhang, X. Zhu, DNA trojan horses: self-assembled floxuridine-containing DNA polyhedra for cancer therapy, Angew. Chem. Int. Ed. Engl. 56 (2017) 12528–12532.

[18] T.B. Nielsen, R.P. Thomsen, M.R. Mortensen, J. Kjems, P.F. Nielsen, T.E. Nielsen, A. B. Kodal, E. Cló, K.V. Gothelf, Peptide-directed DNA-templated Protein labelling for the assembly of a pseudo-IgM, Angew. Chem. Int. Ed. Engl. 58 (2019) 9068–9072.

[19] N. Stephanopoulos, Hybrid nanostructures from the self-assembly of proteins and DNA, Chem 6 (2020) 364–405.

[20] S. Loescher, A. Walther, Supracolloidal self-assembly of divalent Janus 3D DNA origami via programmable multivalent host/guest interactions, Angew. Chem. Int. Ed. Engl. 59 (2020) 5515–5520.

[21] L. Wang, A.M. Urbas, Q. Li, Nature-inspired emerging chiral liquid crystal nanostructures: from molecular self-assembly to DNA mesophase and nanocolloids, Adv. Mater. 32 (2020), e1801335.

[22] D.S. Lee, H. Qian, C.Y. Tay, D.T. Leong, Cellular processing and destinies of artificial DNA nanostructures, Chem. Soc. Rev. 45 (2016) 4199–4225.

[23] Q. Li, J. Zhao, L. Liu, S. Jonchhe, F.J. Rizzuto, S. Mandal, H. He, S. Wei, H. F. Sleiman, H. Mao, C. Mao, A poly(thymine)-melamine duplex for the assembly of DNA nanomaterials, Nat. Mater. 19 (2020) 1012–1018.

[24] H. Li, M. Wang, T.H. Shi, S.H. Yang, J.H. Zhang, H.H. Wang, Z. Nie, A DNA-mediated chemically induced dimerization (D-CID) nanodevice for nongenetic receptor engineering to control cell behavior, Angew. Chem. Int. Ed. Engl. 57 (2018) 10226–10230.

[25] X. Liu, X. Li, J. Liping, G. Cheng, D.T. Leong, Q.W. Xue, 3-D DNA nanodevices for on-site sensitive detection of antibiotic residues in food, Chem. Commun. (2020), https://doi.org/10.1039/d0cc05411a.

[26] P. Song, J. Shen, D. Ye, B. Dong, F. Wang, H. Pei, J. Wang, J. Shi, L. Wang, W. Xue, Y. Huang, G. Huang, X. Zuo, C.H. Fan, Programming bulk enzyme heterojunctions for biosensor development with tetrahedral DNA framework, Nat. Commun. 11 (2020) 838.

[27] A. Chopra, S. Krishnan, F.C. Simmel, Electrotransfection of polyamine folded DNA origami structures, Nano Lett. 16 (2016) 6683–6690.

[28] C. Kielar, Y. Xin, B. Shen, M.A. Kostiainen, G. Grundmeier, V. Linko, A. Keller, On the stability of DNA origami nanostructures in low-magnesium buffers, Angew. Chem. Int. Ed. Engl. 57 (2018) 9470–9474.

[29] J.C.M. Wan, C. Massie, J. Garcia-Corbacho, F. Mouliere, J.D. Brenton, C. Caldas, S. Pacey, R. Baird, N. Rosenfeld, Liquid biopsies come of age: towards implementation of circulating tumour DNA, Nat. Rev. Canc. 17 (2017) 223–238.

[30] H. Qian, C. Tian, J. Yu, F. Guo, M.S. Zheng, W. Jiang, Q.F. Dong, C. Mao, Self-assembly of DNA nanotubes with defined diameters and lengths, Small 10 (2014) 855–858.

[31] K. Ariga, X. Jia, J. Song, J.P. Hill, D.T. Leong, Y. Jia, J.B. Li, Nanoarchitectonics beyond self-assembly: challenges to create bio-like hierarchic organization, Angew. Chem. Int. Ed. Engl. (2020), https://doi.org/10.1002/anie.202000802.

[32] X. Sun, N. Ni, Y. Ma, Y. Wang, D.T. Leong, Retooling cancer nanotherapeutics' entry into tumors to alleviate tumoral hypoxia, Small 16 (2020), e2003000.

[33] M. Ovais, M. Guo, C.Y. Chen, Tailoring nanomaterials for targeting tumor-associated macrophages, Adv. Mater. 31 (2019), e1808303.

[34] B.L. Li, R. Li, H.L. Zou, K. Ariga, N.B. Li, D.T. Leong, Engineered functionalized 2D nanoarchitectures for stimuli-responsive drug delivery, Mater. Horiz. 7 (2020) 455–469.

[35] C. Myhrvold, M. Dai, P.A. Silver, P. Yin, Isothermal self-assembly of complex DNA structures under diverse and biocompatible conditions, Nano Lett. 13 (2013) 4242–4248.

[36] Z. Zhang, J. Song, F. Besenbacher, M. Dong, K.V. Gothelf, Self-assembly of DNA origami and single-stranded tile structures at room temperature, Angew. Chem. Int. Ed. Engl. 52 (2013) 9219–9223.

[37] J. Song, Z. Zhang, S. Zhang, L. Liu, Q. Li, E. Xie, K.V. Gothelf, F. Besenbacher, M. Dong, Isothermal hybridization kinetics of DNA assembly of two-dimensional DNA origami, Small 9 (2013) 2954–2959.

[38] J. Roodhuizen, P. Hendrikx, P.A.J. Hilbers, T. Greef, A.J. Markvoort, Counterion-dependent mechanisms of DNA origami nanostructure stabilization revealed by atomistic molecular simulation, ACS Nano 13 (2019) 10798–10809.

[39] R. Jungmann, T. Liedl, T.L. Sobey, W. Shih, F.C. Simmel, Isothermal assembly of DNA origami structures using denaturing agents, J. Am. Chem. Soc. 130 (2008) 10062–10063.

[40] Z. Zhang, J. Song, F. Besenbacher, M. Dong, K.V. Gothelf, Self-assembly of DNA origami and single-stranded tile structures at room temperature, Angew Chem. Int. Ed. Engl. 52 (2013) 9219–9223.

[41] I. Gállego, M.A. Grover, N.V. Hud, Folding and imaging of DNA nanostructures in anhydrous and hydrated deep-eutectic solvents, Angew. Chem. Int. Ed. Engl. 54 (2015) 6765–6769.

[42] R. Tugyi, K. Uray, D. Iván, E. Fellinger, A. Perkins, F. Hudecz, Partial D-amino acid substitution: improved enzymatic stability and preserved Ab recognition of a MUC2 epitope peptide, Proc. Natl. Acad. Sci. U.S.A. (102) (2005) 413–418.

[43] S. Chen, D. Gfeller, S.A. Buth, O. Michielin, P.G. Leiman, C. Heinis, Improving binding affinity and stability of peptide ligands by substituting glycines with D-amino acids, Chembiochem 14 (2013) 1316–1322.

[44] E.I. Closs, J.P. Boissel, A. Habermeier, A. Rotmann, Structure and function of cationic amino acid transporters (CATs), J. Membr. Biol. 213 (2006) 67–77.

[45] T. Gerling, M. Kube, B. Kick, H. Dietz, Sequence-programmable covalent bonding of designed DNA assemblies, Sci. Adv. 4 (2018), eaau1157.